Representation of the carbon cycle in box models and GCMs: 1. Solubility pump

J. R. Toggweiler, A. Gnanadesikan, and S. Carson
Geophysical Fluid Dynamics Laboratory, NOAA, Princeton, New Jersey, USA

R. Murnane
Risk Prediction Initiative, Bermuda Biological Station for Research, Inc., Garrett Park, Maryland, USA

J. L. Sarmiento
Atmospheric and Oceanic Sciences Program, Princeton University, Princeton, New Jersey, USA

Received 5 March 2001; revised 24 July 2002; accepted 24 October 2002; published 14 March 2003.

[1] *Bacastow* [1996], *Broecker et al.* [1999], and *Archer et al.* [2000] have called attention recently to the fact that box models and general circulation models (GCMs) represent the thermal partitioning of CO_2 between the warm surface ocean and cold deep ocean in different ways. They attribute these differences to mixing and circulation effects in GCMs that are not resolved in box models. The message that emerges from these studies is that box models have overstated the importance of the ocean's polar regions in the carbon cycle. A reduced role for the polar regions has major implications for the mechanisms put forth to explain glacial - interglacial changes in atmospheric CO_2. In parts 1 and 2 of this paper, a new analysis of the ocean's carbon pumps is carried out to examine these findings. This paper, part 1, shows that unresolved mixing and circulation effects in box models are not the main reason for box model-GCM differences. The main factor is very different kinds of restrictions on gas exchange in polar areas. Polar outcrops in GCMs are much smaller than in box models, and they are assumed to be ice covered in an unrealistic way. This finding does not support a reduced role for the ocean's polar regions in the cycling of organic carbon, the subject taken up in part 2. *INDEX TERMS:* 1615 Global Change: Biogeochemical processes (4805); 4267 Oceanography: General: Paleoceanography; 4806 Oceanography: Biological and Chemical: Carbon cycling; 4842 Oceanography: Biological and Chemical: Modeling; *KEYWORDS:* ocean carbon cycle, solubility pump, box model, gas exchange

Citation: Toggweiler, J. R., A. Gnanadesikan, S. Carson, R. Murnane, and J. L. Sarmiento, Representation of the carbon cycle in box models and GCMs: 1. Solubility pump, *Global Biogeochem. Cycles*, *17*(1), 1026, doi:10.1029/2001GB001401, 2003.

1. Introduction

[2] An average water parcel from the deep ocean contains about 2280 μmoles of total CO_2 (TCO_2) per kilogram of seawater. An average parcel of low-latitude surface water contained about 1930 μmoles of TCO_2 per kilogram in preindustrial time. The excess TCO_2 in the deep ocean, i.e., the difference between average deep water and preindustrial surface water, amounted to some 350 μmol/kg, or 15% of the deep concentration. Three factors account for the TCO_2 excess in the deep ocean: (1) The water in the deep ocean is colder and thus can hold more CO_2 at equilibrium with the atmosphere, (2) the deep ocean contains remineralized CO_2 from organic particles that sink from the surface ocean, and (3) the deep ocean contains CO_2 derived from the dissolution of $CaCO_3$ in particles that sink from the surface ocean. Oceanographers refer to these factors as the three carbon "pumps," the solubility pump, the organic or soft tissue pump, and the carbonate pump [*Volk and Hoffert*, 1985].

[3] *Bacastow* [1996], *Broecker et al.* [1999], and *Archer et al.* [2000] have shown recently that carbon cycle models based on general circulation models (GCMs) partition less CO_2 into cold deep waters than do box models. They tend to retain more CO_2 in the atmosphere and low-latitude surface waters. Hence the solubility pump can be said to be weaker or less efficient in GCMs than in box models. This is somewhat surprising as the thermal partitioning of CO_2 would seem to be governed by the solubility of CO_2 in seawater, a thermodynamic property that is independent of model configuration.

[4] Box models tend to feature strong communication between cold water outcrops and the cold water in the interior. *Bacastow* [1996] and *Archer et al.* [2000] argue that this kind of communication unduly favors the partitioning of CO_2 into cold deep water. GCMs, they claim, include circulation and mixing processes that allow the warm surface ocean and cold deep ocean to interact directly.

0886-6236/03/2001GB001401$12.00

Broecker et al. [1999] refine this argument as follows. They claim that the exchange of CO_2 between warm surface waters and cold deep water is more vigorous in the real ocean (and in GCMs) in relation to CO_2 transfer through the atmosphere via gas exchange.

[5] In this and the following paper a new analysis of the ocean's carbon pumps is carried out to examine these arguments. One of the box models and one of the GCMs examined in the *Bacastow* [1996], *Broecker et al.* [1999], and *Archer et al.* [2000] studies are examined here. The three carbon pumps are pulled apart and investigated separately. The solubility pump is examined in part 1 (this paper). The organic pump is examined in part 2 [*Toggweiler et al.*, 2003].

[6] The novel aspect of this analysis is the explicit determination of the gas exchange contribution to each of the carbon pumps. The gas exchange imprint is assessed by running out solubility-only, organic-only, and carbonate-only models with very fast gas exchange. Fast gas exchange brings local CO_2 concentrations into equilibrium with atmospheric CO_2. Thus, CO_2 differences between models with normal gas exchange and fast gas exchange are a measure of the departure from equilibrium in the model with normal gas exchange.

[7] Our analysis shows that box models partition more of their CO_2 into cold deep water because their solutions are closer to thermodynamic equilibrium. GCMs partition less CO_2 into cold deep water because their solutions are further from equilibrium. The source of this disequilibrium is traced to restrictions on gas exchange. The explanation for box model-GCM differences given by *Broecker et al.* [1999] is thus technically correct: The main distinction between box models and GCMs does have to do with the relative vigor of the circulation and gas exchange. The critical factor is not the vigor of the circulation, however; it is restrictions on gas exchange.

2. Separation of the Carbon Pumps

[8] A parcel of seawater at 2°C should contain about 170 μmol/kg more CO_2 than the same parcel at 22°C if both parcels are in chemical equilibrium with the same atmospheric pCO_2 [*Department of Energy*, 1994]. Thus as a first guess, one might expect solubility differences to account for nearly half of the surface to deep difference in TCO_2, i.e., 170 out of 350 μmol/kg. In order for deep water to reach chemical equilibrium, however, it must sink with a pCO_2 equal to that of the atmosphere and warm surface ocean. The key point made by *Broecker et al.* [1999] is that this condition is never achieved in the real ocean. *Broecker et al.* [1999] utilized a particular index called the HBEI, adapted from *Bacastow* [1996], to illustrate how box models and GCMs under perform with respect to full CO_2 solubility.

[9] Here the *Broecker et al.* [1999] argument has been recast in terms of a simpler metric that can be applied to all three carbon pumps. Our metric for the strength the ocean's carbon pumps, individually and together, is simply the TCO_2 difference between cold deep water and warm low-latitude surface water. A series of examples below illustrates how the carbon pumps are separated and how the solubility pump responds in isolation to changes in circulation, mixing, and gas exchange. The examples below are drawn from the three-box model of *Sarmiento and Toggweiler* [1984] and *Siegenthaler and Wenk* [1984] illustrated in Figure 1.

[10] The three-box model contains three ocean boxes coupled to an atmospheric box. The low-latitude surface box (*l*) occupies 85% of the total ocean area while the high-latitude surface box (*h*) occupies the remaining 15%. The rest of the ocean is represented by a very large deep box (*d*). The model has two circulation terms. The "T" circulation moves water up from the deep box into the low-latitude surface box, poleward into the *h* box, and then down again into the deep box. The "f_{hd}" circulation term ventilates the deep box directly through mixing between the high-latitude box and the deep box. T is set to 20 Sv and f_{hd} to 60 Sv. There is no mixing initially between the low-latitude box and the deep box. The temperature of the low-latitude box is set at 21.5°C, while that of the high-latitude box is set at 2.0°C. The water in all three boxes has a salinity of 34.7 psu. Gas exchange is parameterized in terms of a piston velocity of 3 m/day in both surface boxes.

[11] Biological activity in the model is specified in terms of the sinking particle fluxes P_l and P_h. The sinking flux from the low-latitude box, P_l, is set equal to the PO_4 input to the box with PO_{4l} set equal to zero. The high-latitude sinking flux, P_h, is set to a constant value, 0.00615 moles $P/m^2/yr$ (equivalent to a flux of 1 mole of carbon per square meter per year). The amount of organic carbon in the sinking flux is given in terms of a C:P ratio, $r_{Corg:P}$ = 130:1. Twenty percent of the carbon in the sinking flux is assumed to be $CaCO_3$. Thus, the total C flux per mole P, $r_{C:P}$, is $130/(1 - 0.2) = 162.5$. For more details, see *Toggweiler* [1999].

[12] The three ocean boxes are initialized with the observed global mean PO_4, 2.09 μmol/kg, and alkalinity, 2371 μeq/kg (after Table 2 of *Toggweiler and Sarmiento* [1985]). The three oceanic boxes are then given a first guess TCO_2 concentration and the model is run out to steady state. The initial TCO_2 is then adjusted by trial and error until the pCO_2 in the atmospheric box falls into the narrow range of 280 ± 0.2 ppm. The TCO_2 used to initialize the three ocean boxes with normal gas exchange is 2249.4 μmoles/kg.

[13] The solution for the full model (all three pumps combined) is given in the first column of Table 1. The TCO_2 concentration in the deep box is 2258 μmol/kg. This is very close to the average TCO_2 for the whole ocean. The TCO_2 of the low-latitude surface box is 1926 μmol/kg. The TCO_2 difference between the deep box and the low-latitude surface box is 332.2 μmol/kg as shown in bold type at the bottom of Table 1.

[14] Two versions of the model are run out. Version 1 uses the standard gas exchange piston velocity of 3 m/day. Version 2 uses a fast piston velocity of 90 m/day, 30 times larger than the standard value. The solution for Version 2 is given in the second column of Table 1. The TCO_2 difference between the deep box and low-latitude surface box is 329.7 μmol/kg with fast gas exchange, not appreciably different from the TCO_2 difference in the model with normal gas exchange.

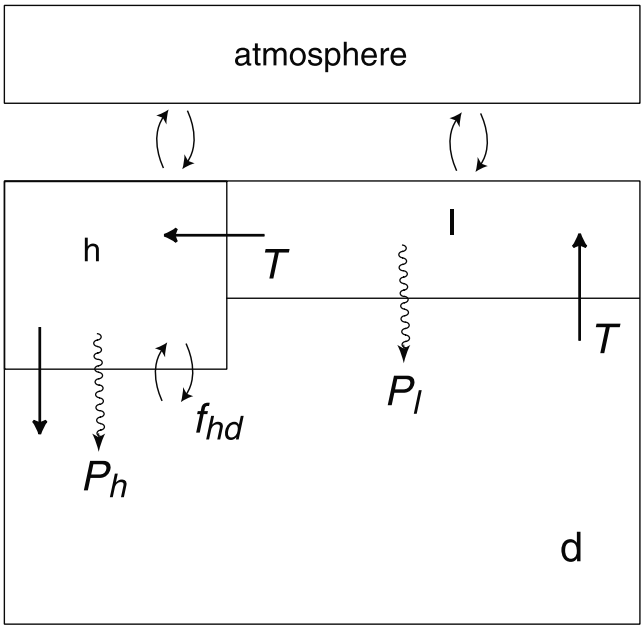

Figure 1. Schematic diagram of the three-box model of *Sarmiento and Toggweiler* [1984] and *Siegenthaler and Wenk* [1984].

[15] Solubility-only versions of the three-box model are initialized and run in the same way as the full model but with all biological fluxes switched off. TCO_2 concentrations used to initialize the solubility-only models with normal and fast gas exchange are 2154.5 and 2170.6 μmoles/kg, respectively. Solubility-only results are given in columns three and four of Table 1. The TCO_2 difference between the deep box and low-latitude surface box is 141.1 μmol/kg with normal gas exchange and 164.7 μmol/kg with fast gas exchange.

[16] To separate the organic and carbonate pumps from the solubility pump, the temperatures of the two surface boxes are set to 10°C. This means that all the water in the model has the same temperature. The organic pump is then separated from the carbonate pump by setting the carbonate fraction of the sinking flux to zero. TCO_2 concentrations used to initialize the organic-only models with normal and fast gas exchange are 2223.7 and 2199.7 μmoles/kg, respectively. Output from organic-only models is given in columns five and six of Table 1. The cycling of organic matter can be seen to be the same as in the full model: The PO_4 distribution is the same and the oxygen deficit in the deep box is also the same; that is, $AOU_d - AOU_h = 111.7$ μmol/kg. Alkalinities in the three ocean boxes do not change from the initial condition.

[17] To separate the carbonate pump from the organic pump, the uptake and remineralization of TCO_2 is reduced to the carbonate fraction; that is, $r_{Corg:P} = 0$ and $r_{C:P} = 162.5 \times 0.2$. Columns seven and eight in Table 1 give results for the two versions of the carbonate-only model with normal and fast gas exchange. Note that alkalinity values in the carbonate-only models are the same as in the full model.

[18] A key test of the pump separation is a demonstration that the surface to deep TCO_2 differences due to the three pumps can be added together to yield the surface to deep TCO_2 difference in the full model. Table 2 summarizes these differences for the solubility-only, organic-only, and the carbonate-only results from Table 1. Surface to deep TCO_2 differences for the three separated pumps can be combined to yield an overall surface to deep TCO_2 difference of 339.6 μmol/kg with normal gas exchange. This sum is 7 μmol/kg higher than the surface to deep TCO_2 differ-

Table 2. Sum of Surface to Deep TCO_2 Differences Across the Three Pumps

	Normal Gas Exchange	Fast Gas Exchange
Solubility pump	141.7 μmol/kg	164.7 μmol/kg
Organic pump	116.7	87.2
Carbonate pump	81.8	84.1
Sum	**339.6**	**336.0**
Full model	**332.2**	**329.7**

Table 1. Surface to Deep TCO_2 Differences in the Three-Box Model

		Full Model		Solubility-Only		Organic-Only		Carbonate-Only	
Model Variable	Units	Standard Gas Exchange	30x Gas Exchange	Standard Gas Exchange	30x Gas Exchange	Standard Gas Exchange	30x Gas Exchange	Standard Gas Exchange	30x Gas Exchange
PO_{4l}	μmol/kg	0		2.090		0		0	
PO_{4h}	μmol/kg	1.485		2.090		1.485		1.485	
PO_{4d}	μmol/kg	2.146		2.090		2.146		2.146	
Alk_l	μeq/kg	2266.5		2371.0		2371.0		2266.5	
Alk_h	μeq/kg	2340.8		2371.0		2371.0		2340.8	
Alk_d	μeq/kg	2373.8		2371.0		2371.0		2373.8	
TCO_{2l}	μmol/kg	1925.9	1926.5	2016.6	2009.7	2110.6	2115.4	2027.6	2027.4
TCO_{2h}	μmol/kg	2150.7	2148.8	2157.7	2174.4	2141.3	2116.7	2087.9	2090.0
TCO_{2d}	μmol/kg	2258.1	2256.2	2157.7	2174.4	2227.2	2202.6	2109.4	2111.5
pCO_{2atm}	ppm	280.1	279.9	280.2	279.9	280.1	280.0	279.9	280.0
pCO_{2l}	ppm	279.1	279.9	289.0	280.2	272.9	279.7	280.4	280.0
pCO_{2h}	ppm	283.2	280.0	253.5	280.2	320.7	281.6	276.9	279.8
O_{2d}	μmol/kg	217.1	220.6	331.6	332.3	160.9	163.3	275.4	275.4
AOU_h	μmol/kg	4.0	0.6	1.2	0.2	2.7	0.4	0	0
AOU_d	μmol/kg	115.8	112.3	1.2	0.2	114.4	112.1	0	0
$TCO_{2d} - TCO_{2l}$	μmol/kg	**332.2**	**329.7**	**141.1**	**164.7**	**116.7**	**87.2**	**81.8**	**84.1**

ence in the full model, 332.2 μmol/kg. One sees a similar result in the models with fast gas exchange. One does not expect the effects of the three pumps to be additive in a perfectly linear way. The comparison in Table 2 shows, however, that the combined effect of the three separated pumps is a close approximation to the behavior of the full model.

3. Solubility Pump in the Three-Box Model

3.1. Solubility-Only Model With Normal and Fast Gas Exchange

[19] Figure 2 presents the solubility-only results from Table 1 in a more accessible form. The top panel gives results from the standard solubility-only model with normal gas exchange. TCO_2 concentrations (in μmol/kg) are shown within each box while the pCO_2 in each surface box (in ppm) is given just above. The strength of the solubility pump, $TCO_{2d} - TCO_{2l}$, is given to the right of each diagram. As noted above, the surface to deep TCO_2 difference in the solubility-only model with normal gas exchange is 141 μmol/kg. TCO_2 concentrations in the deep box and the high-latitude box are identical because water from the high-latitude box fills the deep box without being altered.

[20] The pCO_2 of the low-latitude box in the standard solubility-only model is 9 ppm higher than the atmospheric pCO_2 while the pCO_2 of the high-latitude box is 26 ppm lower. This sort of result is expected from the cycle of heating and cooling in the model. The air-sea pCO_2 differences in the two surface boxes have a direct effect on the strength of the solubility pump and the amount of CO_2 that the ocean can hold. A low pCO_2 in the high-latitude box reduces the amount of CO_2 in the high-latitude and deep boxes and thereby reduces $TCO_{2d} - TCO_{2l}$. An elevated pCO_2 in the low-latitude surface box increases the amount of CO_2 in the low-latitude box and also reduces $TCO_{2d} - TCO_{2l}$. Large air-sea pCO_2 differences mean that the deep ocean will hold less CO_2 for a given surface to deep temperature difference.

[21] The second panel of Figure 2 gives results from the solubility-only model with fast gas exchange. With a piston velocity of 90 m/day the transfer of CO_2 between the surface boxes and the atmosphere is sufficiently fast that the pCO_2 in each surface box is within 1 ppm of the atmospheric value. This raises the TCO_2 of the deep box and lowers the TCO_2 of the low-latitude surface box and brings the surface to deep TCO_2 difference up to 165 μmol/kg. This is the TCO_2 difference expected in the box model at full thermodynamic equilibrium. The surface to deep TCO_2 difference at full solubility is half the surface to deep TCO_2 difference in the full model, 165 versus 330 μmol/kg.

[22] The difference between the surface to deep TCO2 differences in the models with normal and fast gas exchange is 165 − 141 = 24 μmol/kg. This difference is the departure from equilibrium of the solubility pump in the model with normal gas exchange.

3.2. Solubility-Only Model With Fast Circulation

[23] The third panel of Figure 2 gives results for a version of the solubility-only model in which the overturning T circulation is increased by a factor of 2 from 20 to 40 Sv while the gas exchange piston velocity in the two surface boxes is held fixed at 3 m/day. A faster T circulation causes the pCO_2 in the low-latitude box to increase to 295 ppm and the pCO_2 of the high-latitude box to decrease to 234 ppm. With larger air-sea pCO_2 differences, the strength of the solubility pump is reduced from 141 to 122 μmol/kg.

[24] This result illustrates one of the ways in which *Broecker et al.* [1999] expected GCMs to differ from box models. Broecker et al. argued that more physical exchange

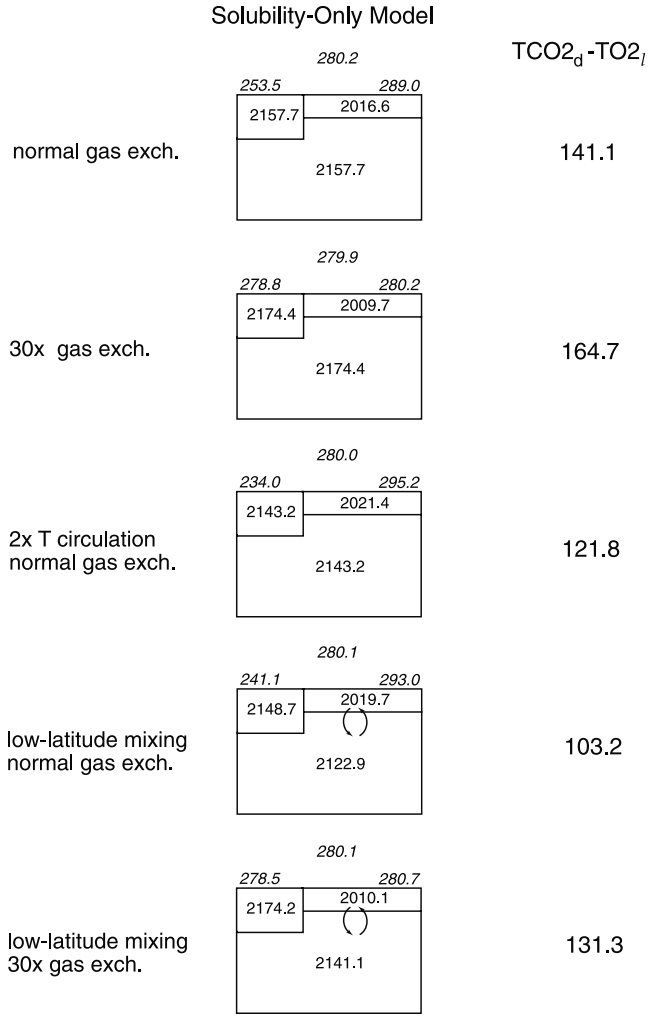

Figure 2. TCO_2 concentrations and pCO_2s for five solubility-only solutions of the three-box model. The top two panels give results from the standard model with normal gas exchange and fast (30x) gas exchange. The middle panel gives output from a model in which the T circulation is doubled to 40 Sv with normal gas exchange. The bottom two panels give results from a model with an additional 20 Sv of mixing between the low-latitude box and the deep box. TCO_2 concentrations are given inside the boxes in μmol/kg. The pCO_2 of the two ocean surface boxes are given just above; the atmospheric pCO_2 is given in the middle (units 10^{-6} atm or ppm). The TCO_2 difference between the deep box and low-latitude surface box is given to the right.

between warm low-CO_2 upper ocean waters and cold high-CO_2 deep waters in GCMs should increase the departure from full solubility. The results in the middle panel of Figure 2 support that view. An enhanced T circulation means that the water in the two surface boxes is warmed and cooled at greater rates. Increased rates of heating and cooling in relation to a fixed gas exchange rate increase pCO_2 differences between the ocean and atmosphere. This causes the surface to deep difference in TCO_2 to depart more strongly from equilibrium. Halving the gas exchange rate with T held at 20 Sv reduces the solubility pump by the same amount as a doubling of the overturning rate. Doubling the T circulation in a model with fast gas exchange has no effect because surface CO_2 concentrations remain at equilibrium with the atmospheric pCO_2.

[25] A doubling of the T circulation reduces the strength of the solubility pump by 19 μmol/kg. This will turn out to be a very modest reduction in relation to the surface to deep TCO_2 differences in the GCM to be examined below. A stronger circulation, by itself, is unlikely to explain a large departure from equilibrium.

3.3. Effect of Mixing Between the Low-Latitude and Deep Boxes

[26] The bottom two panels of Figure 2 give results from a pair of solubility-only models in which an extra mixing term is added between the low-latitude and deep boxes. The new mixing term, "f_{ld}," is given a magnitude of 20 Sv, the same as T. One expects the deep box in a model with low-latitude mixing to be warmer and to hold less CO_2. Indeed, mixing between the deep box and the low-latitude box in this example increases the temperature of the deep box to 5.9°C in relation to the 2.0°C temperature in the high-latitude box. The surface to deep TCO_2 difference in the model with normal gas exchange is reduced from 141 to 103 μmol/kg. The surface to deep TCO_2 difference with fast gas exchange is reduced from 165 to 131 μmol/kg. Similar reductions with the two different gas exchange rates are not unexpected as the warming effect of low-latitude mixing should be the same whether gas exchange rates are fast or slow.

[27] Low-latitude mixing reduces the surface to deep TCO_2 difference by a slightly larger amount with normal gas exchange, 38 μmol/kg, than with fast gas exchange, 34 μmol/kg. This comes about because of a secondary effect that is independent of warming. Mixing between the low-latitude box and the deep box causes TCO_2 concentrations in the warmer deep box to decrease in relation to TCO_2 concentrations in the high-latitude surface box. Mixing between the deep box and the high-latitude surface box, i.e., f_{hd}, then acts to reduce the TCO_2 of the high-latitude box and to pull the pCO_2 of the high-latitude box away from the atmospheric pCO_2. This aspect of mixing enhances the air-sea pCO_2 difference in the polar box and weakens the solubility pump in the same manner as an enhanced T circulation.

3.4. Abiotic pCO_2 With Fast Gas Exchange

[28] *Archer et al.* [2000] introduced a metric called the abiotic pCO_2 to evaluate the solubility pump in a number of box models and GCMs. To determine the abiotic pCO_2, a solubility-only model is initialized with alkalinity and TCO_2 concentrations of 2371 μeq/kg and 2085 μmol/kg, respectively, and run to steady state. The abiotic pCO_2 is the atmospheric pCO_2 derived from those initial conditions. A model with a low abiotic pCO_2 partitions more of its initial CO_2 into the cold deep ocean. It therefore has a large TCO_2 difference between its warm surface water and cold deep water. The standard three-box model in this paper has an abiotic pCO_2 of 211 ppm. (The abiotic pCO_2 of 211 ppm determined here is lower than the 219 ppm figure given for the three-box model by *Archer et al.* [2000] because the three-box model used here has no mixing between the low- and high-latitude surface boxes and no mixing between the low-latitude surface box and the deep box.) The surface to deep TCO_2 difference in this model is 143 μmol/kg, not unlike the result in Figure 2 derived with a 280-ppm atmosphere.

[29] *Archer et al.* [2000] determined the abiotic pCO_2 in a number of GCMs and found that the abiotic pCO_2 in these models ranged between 250 and 290 ppm. These results were distinctly different from the abiotic pCO_2 in a set of four box models which fell in the low two hundreds. Archer et al. did not reference their results to equilibrium, however, by evaluating their abiotic pCO_2s with fast gas exchange. Had they done so they would have seen that all their models are alike at this limit. Each model would have an abiotic pCO_2 close to 200 ppm with fast gas exchange: The particular value would depend on the equilibrium constants being used and the model's thermal structure. The three-box model with 30x gas exchange has an abiotic pCO_2 of 189 ppm.

[30] *Archer et al.* [2000] viewed the spread in abiotic pCO_2 between their box models and GCMs as an expression of stronger circulation or mixing effects in the GCMs, but they did not ask whether gas exchange differences might also be a factor. As will be shown below, the abiotic pCO_2s in the GCMs examined by Archer et al. are high because CO_2 concentrations in these models are far from chemical equilibrium. Finite gas exchange does not allow the TCO_2 concentrations in deep water in these models to come anywhere close to equilibrium.

4. Solubility Pump in the Princeton Ocean Biogeochemistry Model (POBM)

[31] The Princeton Ocean Biogeochemistry Model (POBM) is one of the GCMs examined by *Broecker et al.* [1999] and *Archer et al.* [2000]. A full description of the POBM is given by *Murnane et al.* [1999]. As part of their study, Murnane et al. ran out two solubility-only solutions to look at the impact of gas exchange on solubility effects. Murnane et al.'s solubility-only solutions are prototypes for the calculations carried out in the present study.

[32] The POBM is derived from a GCM based on the Geophysical Fluid Dynamics Laboratory Modular Ocean Model (GFDL MOM) version 1. The model solves a three-dimensional equation for momentum and conservation equations for temperature and salinity. It is built on a coarse grid (4.5° latitude by 3.75° longitude with 12 vertical levels). The maximum depth is 5000 m. The model uses the *Bryan and Lewis* [1979] vertical mixing scheme in

which vertical mixing varies with depth from 0.3 cm^2/s in the upper kilometer to 1.3 cm^2/s in the lower kilometer. Horizontal mixing is oriented along level horizontal surfaces. The surface wind stress and the surface forcing for temperature and salinity are derived from annual mean fields.

[33] The full POBM includes additional tracers for phosphate (PO_4), oxygen, total alkalinity, dissolved inorganic carbon (DIC), and dissolved organic carbon (DOC). For the runs considered here, all biological fluxes were turned off and alkalinity was treated as a conservative tracer that varies with salinity. The TCO_2 distribution was then allowed to evolve under a fixed preindustrial atmosphere. This solution is called the solubility model in the *Murnane et al.* [1999] paper. In a second solubility-only simulation, called the potential solubility model, the pCO_2 in every surface grid cell was restored at every time step to the preindustrial value as a way of simulating fast gas exchange.

[34] Figure 3 shows average vertical profiles of TCO_2 from the *Murnane et al.* [1999] solubility and potential solubility models. Surface TCO_2 concentrations in the two profiles are similar. Deep TCO_2 concentrations are quite different. One can see immediately that the strengths of the solubility pumps in these models are very different. Deep water in the model with normal gas exchange has about 75 μmoles/kg less TCO_2 than expected at equilibrium! This is a much larger departure from equilibrium than was seen in any of the box-model illustrations in the previous section.

[35] To make a direct comparison with a box model, one needs to identify a volume of low-latitude surface water that has the same average temperature as the low-latitude box in the box model and a volume of deep water with the same average temperature as the deep box. One must also normalize the average TCO_2 concentrations in these volumes to the same salinity. The salinity normalized TCO_2 difference between these volumes should then be directly comparable to TCO_2 differences in the box model. The appropriate volumes in the POBM are the model's surface layer between 50°N and 50°S with an average temperature of 21.52°C, and the volume of ocean below 2000 m with an average temperature of 1.80°C.

[36] Table 3 lists the pertinent results from the POBM. The average surface TCO_2 between 50°N and 50°S in *Murnane et al.*'s [1999] solubility model is 2006 μmol/kg. The corresponding figure for the potential solubility model is 1998 μmol/kg. Average TCO_2 concentrations below 2000 m are 2104 and 2174 μmol/kg, respectively. Surface to deep TCO_2 differences are given in the bottom row of Table 3 after individual TCO_2 concentrations are normalized to 34.7 psu. Salinity-normalized surface to deep TCO_2 differences are thus 122 and 199 μmol/kg, respectively. The spread or departure from equilibrium in the model with normal gas exchange is 77 μmol/kg.

[37] Before the departure from equilibrium is examined in more detail, it is important to point out that the surface to deep TCO_2 difference in the *Murnane et al.* [1999] potential solubility model, 199 μmol/kg, is much larger than the surface to deep TCO_2 difference, 165 μmol/kg, in the three-box model with fast gas exchange. This is somewhat disturbing as both solutions should be at full solubility with more-or-less the same surface and deep temperatures. This difference has been investigated and traced to four factors. One is the set of equilibrium constants being used. If the set of constants used in the box model is replaced by the set used in the GCM, the surface to deep TCO_2 difference at full solubility increases from 165 to 182 μmol/kg. The POBM also has salinity differences whereas the basic box model has none, and it accounts for the effect of water vapor in the air when air-sea pCO_2 differences are determined. Deep water below 2000 m is also slightly cooler than the deep box of the box model. When all these effects are accounted for, the surface to deep TCO_2 difference in the box model increases to 193 μmol/kg at full solubility in much better agreement with the Murnane et al. result.

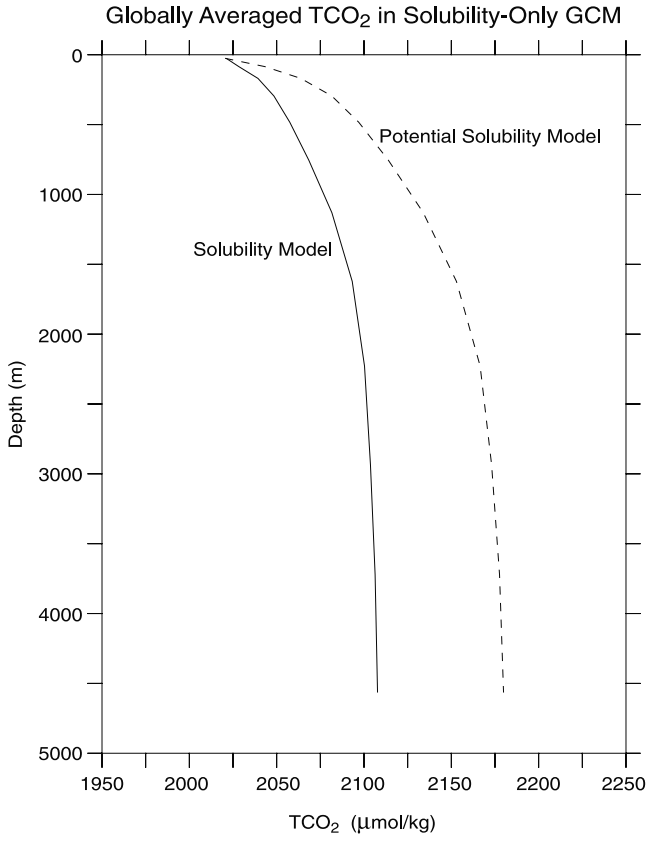

Figure 3. Globally averaged TCO_2 profiles in the Princeton Ocean Biogeochemistry Model (POBM) (units μmol/kg) [*Murnane et al.*, 1999]. The solid curve shows results from Murnane et al.'s solubility model with normal gas exchange rates. The dashed curve shows results from their potential solubility model in which the pCO_2 in every surface grid box is continuously restored to the pCO_2 of the preindustrial atmosphere as a way of simulating fast gas exchange.

5. Restricted Polar Areas and Sea Ice Inhibition

[38] The large solubility differences between the three-box model and the POBM can be traced to two factors, (1) the relatively small area of polar outcrops in the GCM in

Table 3. Surface to Deep TCO_2 Differences in Solubility-Only Versions of the Princeton Ocean Biogeochemistry Model

	Solubility Model	Potential Solubility Model
Average Surface Properties 50°N–50°S		
Temperature	21.52°C	21.52°C
Salinity	35.042 psu	35.042 psu
$TCO_{2\ Surf}$	2005.7 μmol/kg	1997.9 μmol/kg
$TCO_{2\ Surf}$ @34.7 psu	1986.2	1978.4
Average Properties 2000–5000 m		
Temperature	1.80°C	1.80°C
Salinity	34.642 psu	34.642 psu
$TCO_{2\ Deep}$	2104.4 μmol/kg	2174.0 μmol/kg
$TCO_{2\ Deep}$ @34.7 psu	2107.9	2177.7
($TCO_{2\ Deep}$ − $TCO_{2\ Surf}$) @ 34.7 psu	**121.7** μmol/kg	**199.3** μmol/kg

relation to the large polar box in the three-box model and (2) the way that sea ice is assumed to inhibit gas exchange in the GCM. This discussion begins with an illustration of the polar area effect in the three-box model.

[39] The high-latitude box of the three-box model occupies 15% of the ocean's total area. This particular figure was selected in the original version of the model because it represents the area of the Southern Ocean and North Atlantic with unutilized nutrients. Figure 4 shows the strength of the solubility pump ($TCO_{2d} - TCO_{2l}$) for a series of model runs in which the high-latitude area is reduced from 21% of the total ocean area down to 15% and then down to 1.5%. Results for the standard model with a 15% polar area are given along the vertical dashed line on the right-hand side of the plot. The total amount of CO_2 in the ocean-atmosphere system was held constant for the model runs in Figure 4.

[40] The strength of the solubility pump in Figure 4 decreases as the area of the polar box is reduced. The weakening pump is reflected here in a rising atmospheric pCO_2 and a decrease in $TCO_{2d} - TCO_{2l}$. The key variable in this illustration is the pCO_2 deficit in the high-latitude surface box ($pCO_{2atm} - pCO_{2h}$, the lower curve in Figure 4) which increases as the area of the polar box is reduced in the same way that the atmospheric pCO_2 increases. When the pCO_2 deficit in the polar box is large, more of the CO_2 in the system remains in the atmosphere and low-latitude surface ocean and less is partitioned into the deep box.

[41] The result in Figure 4 reflects a changing competition between gas exchange and circulation in the spirit of *Broecker et al.* [1999]. There is a new twist, however, as the response to reduced polar area is exponential at low polar areas. There is relatively little response to the polar area until the area drops below 8 or 9%. Below 4 or 5% the surface to deep TCO_2 difference drops off rather precipitously. The accelerated response at low polar area is a consequence of the fact that the cooling rate in the polar box, dictated by the magnitude of T and the volume of the box, is increasing at the same time that the area available for gas exchange is being reduced. Thus, a small polar area is seen to greatly exacerbate the effect of finite gas exchange rates.

[42] The surface to deep TCO_2 difference in the POBM was shown in the previous section to be about 75 μmol/kg less than at equilibrium. This level of disequilibrium is encountered in Figure 4 below the drop-off point where $TCO_{2d} - TCO_{2l}$ is about 90 μmol/kg; that is, 165 − 75 = 90 μmol/kg. The polar area in the box model corresponding to this level of disequilibrium is just below 3%. The vertical dashed line on the left-hand side of Figure 4 highlights box model results with a polar area of 3%. The high-latitude pCO_2 deficit at this level of disequilibrium is between 90 and 100 ppm.

[43] Figure 5 examines the relationship between polar area and pCO_2 deficit in the POBM. The top panel of Figure 5 shows air-sea CO_2 fluxes in the *Murnane et al.* [1999] solubility model. The bottom panel is a map of the sea−air pCO_2 differences. CO_2 fluxes in low latitudes (top panel) are directed out of the ocean (negative contours). CO_2 fluxes poleward of 40° latitude are generally into the ocean. Much of the flux in the high-latitude areas is concentrated in a few high-flux regions (>4 moles C/m^2/yr) in the North Atlantic and Southern Ocean. The high flux areas have large pCO_2 deficits in excess of 70 ppm. CO_2 also enters the ocean at lower rates around the perimeter of Antarctica where pCO_2 deficits are as large as 100 ppm.

[44] The high-flux/high pCO_2-deficit regions in the Southern Ocean in Figure 5 are areas of deep convection. Thus, much of the solubility-induced CO_2 uptake in the POBM is seen to occur in isolated regions of limited area where subsurface water is brought to the surface and cooled during a short period of time. The area of the ocean occupied by these areas is much smaller than the area of the ocean with unutilized nutrients. In fact, the area occupied by the high-flux/high pCO_2-deficit regions in the POBM is roughly 15×10^{12} m^2, about 4% of the overall surface area in the POBM. On this point, the three-box model and the POBM seem to be in agreement: The departure of the POBM from equilibrium is consistent with the departure in the box model when the cold water that fills the deep ocean in both models comes into contact with the atmosphere through a small area.

[45] Gas exchange rates in the POBM are also reduced in areas where sea ice is assumed to limit gas exchange. The limitation is proportional to the number of months of the year that a given area is ice covered in sea-ice climatologies. Low gas exchange rates compound the effect of small outcrop areas. The sea-ice inhibition is especially pronounced in the Weddell and Ross Seas where pCO_2 deficits up to 100 ppm are seen in Figure 5. It is these large ice-influenced pCO_2 deficits that kick the POBM's deep-water disequilibrium up to 75 μmol/kg.

[46] In pointing to the competition between gas exchange and circulation as the explanation for box model - GCM differences, *Broecker et al.* [1999] anticipated that GCMs would be different because of a faster or better resolved circulation. Circulation or mixing differences need not be invoked to explain the smaller surface to deep TCO_2 differences in the POBM. The POBM is different because the polar outcrops in the GCM occupy a small surface area and key polar areas are assumed to be partially ice covered. Although only one of the GCMs examined by *Broecker et al.* [1999] and *Archer et al.* [2000] has been examined here, it is possible that restricted

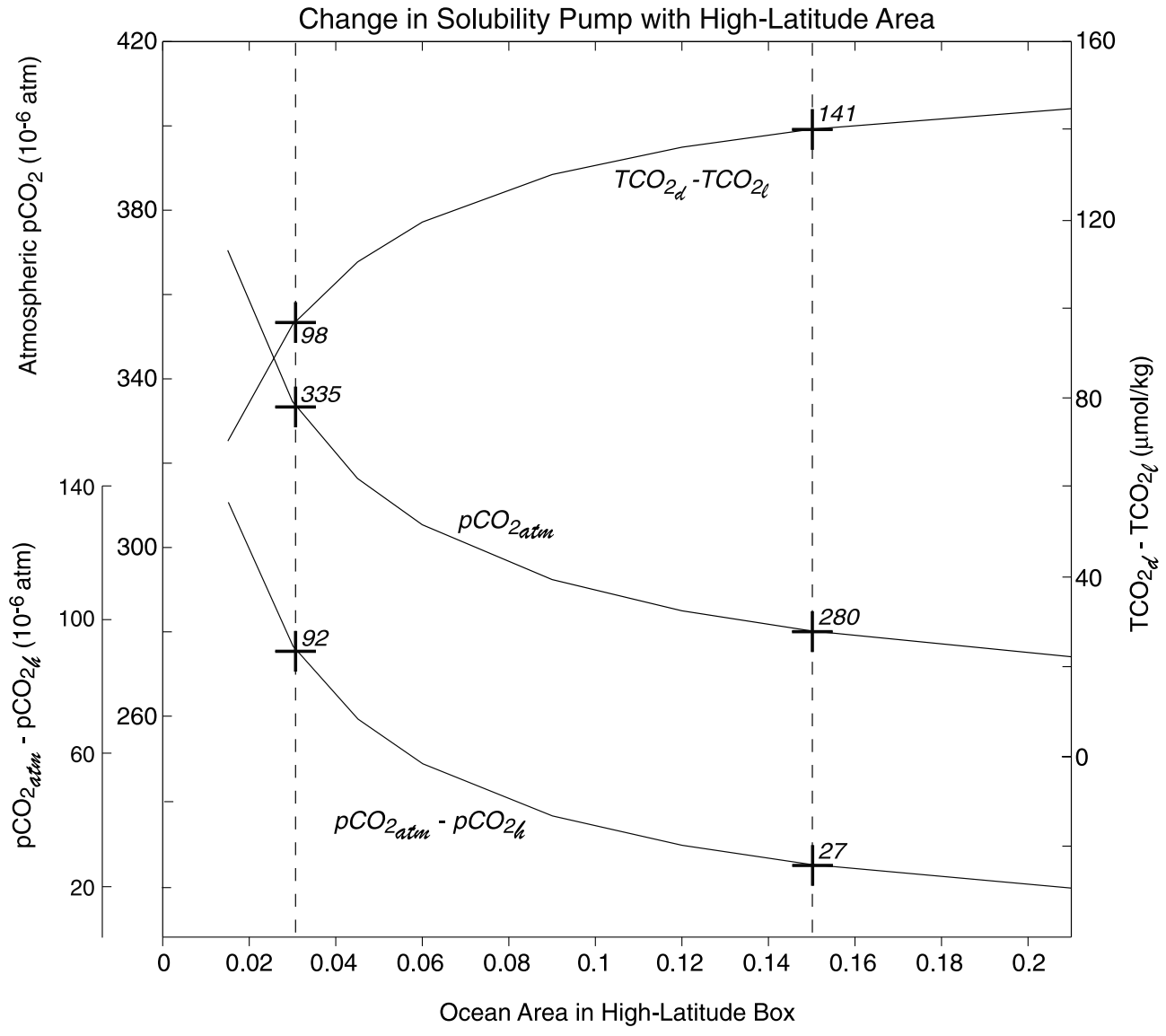

Figure 4. Solubility pump strength, $TCO_{2d} - TCO_{2l}$ (μmol/kg), atmospheric pCO_2 (10^{-6} atm), and high-latitude pCO_2 deficit, $pCO_{2atm} - pCO_{2h}$ (10^{-6} atm), as a function of high-latitude area in the standard three-box model. The strength of the solubility pump decreases with reduced polar area. The vertical dashed lines highlight results with a 3% polar area and 15% polar area.

gas exchange may explain the large departures from equilibrium in all of them.

6. Discussion

6.1. Solubility-Induced pCO_2 Deficits in the Real Ocean

[47] The relatively well equilibrated deep water in the deep box of the three-box model can be attributed to the small pCO_2 deficit that is carried into the interior when new deep water is formed in the polar box. The poorly equilibrated deep water in the POBM can be attributed to the large polar pCO_2 deficits seen in Figure 5. So, which solubility state is more like the solubility state of the real ocean? Essentially, what is the average pCO_2 deficit carried into the interior when deep water forms in the real ocean?

[48] This question does not have an easy answer because the solubility-induced pCO_2 deficit in the real ocean is not easily separated from ΔpCO_2 contributions due to other carbon cycle components [*Gruber and Sarmiento*, 2002]. In particular, solubility-induced pCO_2 deficits tend to be masked by sea-air pCO_2 surpluses that arise from CO_2 that has been remineralized from organic particles [*Murnane et al.*, 1999; *Sarmiento et al.*, 2000]. In this section of the paper we will try to adjudicate between the contrasting solubility states of the two models by developing an independent estimate for the solubility-induced pCO_2 deficit in the real ocean.

[49] Solubility-induced CO_2 uptake is driven mainly by the high-latitude cooling that occurs when surface and thermocline waters move laterally from a warm part of the ocean to a cold part. A pCO_2 deficit is generated because

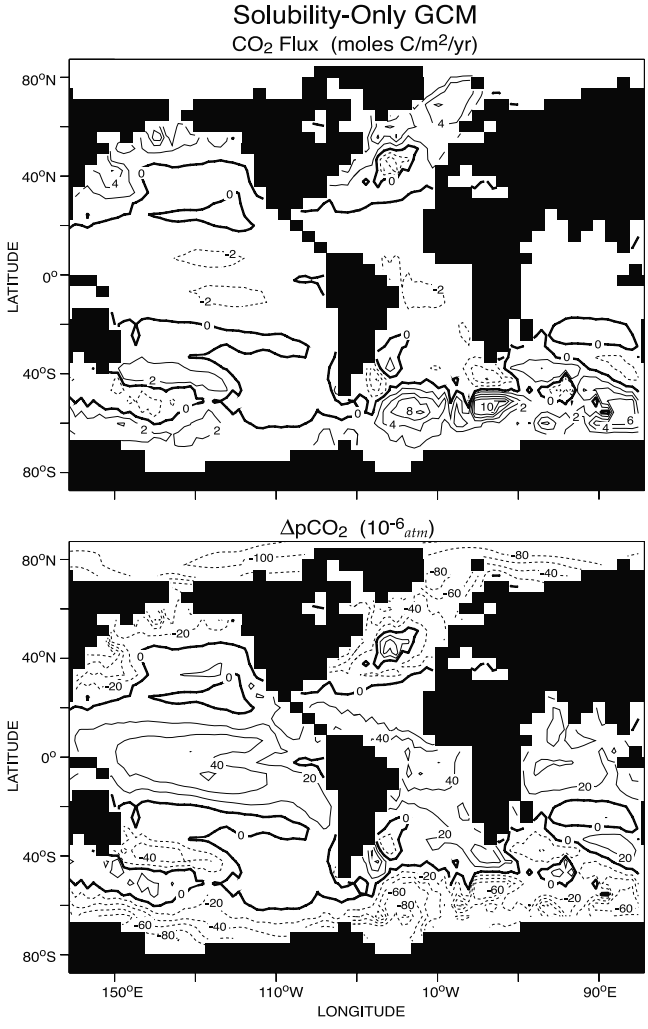

Figure 5. (top) Air-sea CO_2 fluxes in the solubility-only version of the POBM [from *Murnane et al.*, 1999]. Contour interval is 2 moles C/m^2/yr. Positive fluxes indicate that CO_2 is going into the ocean. A color version of this figure is given by *Sarmiento et al.* [2000, Plate 1]. A zonally integrated version of this field is plotted as the solubility model result of *Murnane et al.* [1999, Figure 6]. (bottom) Sea−air pCO_2 differences from the solubility-only POBM (units 10^{-6} atm). Negative contours denote areas where the oceanic pCO_2 is less than atmospheric. Fluxes of CO_2 into the ocean in the top panel tend to be concentrated in small areas with large pCO_2 deficits where convection is active.

the relatively slow air-sea equilibration process does not keep pace with the cooling [*Sarmiento et al.*, 2000]. The most critical part of this transition should be the last stage where the local pCO_2 gradient between the ocean and atmosphere determines the TCO_2 concentration that is carried into the interior.

[50] The North Atlantic is, by far, the most important area of the ocean in terms of high-latitude cooling. *Takahashi et al.* [1995] have compiled seasonally averaged records of sea−air pCO_2 differences in the North Atlantic from which they constructed maps of CO_2 fluxes. Takahashi et al. found that pCO_2 deficits in the North Atlantic extend from 15°N into the Arctic Ocean. The pCO_2 deficits in the southern half of this region reflect CO_2 uptake that is balancing CO_2 outgassing in the tropics. Deficits north of 40°N are more directly attributable to the cooling and poleward advection associated with deep-water formation. The average pCO_2 deficit is about 60−70 ppm during the winter in the region north of Iceland where the densest North Atlantic Deep Water (NADW) is formed [*Weiss et al.*, 1992; *Takahashi et al.*, 1995]. The pCO_2 deficit north of Iceland is larger during the summer due to biological activity.

[51] The wintertime pCO_2 deficit north of Iceland (60−70 ppm) will be taken as a starting point for estimating the average solubility-induced pCO_2 deficit carried into the deep ocean. It is noteworthy in this regard that the observed wintertime pCO_2 deficits north of Iceland agree very well with the solubility-only deficits north of Iceland in the POBM (Figure 5). Low concentrations of remineralized nutrients in the subsurface waters north of Iceland suggest that the observed deficit should not be strongly affected by the outgassing of remineralized CO_2.

[52] The colder bottom waters forming in the Southern Ocean should increase the average TCO_2 concentration for the deep ocean as a whole. The more relevant question is: How does deep-water formation in the Southern Ocean shift the mean pCO_2 deficit in relation to the pCO_2 deficit being set in the North Atlantic? The observed surface pCO_2 distribution is not of much use here because the outgassing of remineralized CO_2 in the Southern Ocean tends to overwhelm the solubility-induced CO_2 uptake. Southern deep-water formation in the POBM introduces a larger pCO_2 deficit into the deep ocean (Figure 5). It is unlikely that this is true in the real ocean.

[53] The major site of dense-water formation in the North Atlantic, the Norwegian Atlantic Current, is an area of intense local cooling [*Mauritzen*, 1996]. Northern cooling is intense because the precursor water masses for NADW are warm water masses from the near-surface and thermocline layers of the North Atlantic that must be cooled by more than 10°C [*Schmitz and Richardson*, 1991]. The main precursor for Antarctic Bottom Water (AABW) is Circumpolar Deep Water (CDW) [*Orsi et al.*, 1999]. CDW has a temperature of only 1.5°C and is only a few degrees warmer than AABW. Thus, the precursors of AABW must be cooled very little in relation to the precursors of NADW.

[54] The conversion of CDW into bottom water takes place in two stages. The first takes place in the open ocean, the second on the Antarctic continental shelves. Isopycnals associated with CDW rise south of the Antarctic Circumpolar Current so that CDW is found at relatively shallow depths (200−600 m) next to Antarctica. Contact between the atmosphere and CDW is blocked by the overlying Antarctic pycnocline but CDW is known to mix with remnant winter mixed-layer water as it is absorbed upward into the pycnocline [*Martinson and Ianuzzi*, 1998]. It is this blend of CDW and winter surface water that flows onto the Antarctic continental shelves [*Jacobs et al.*, 1985; *Foldvik et al.*, 1985]. The modified CDW that finally reaches the Antarctic shelves is very cold, −1.0°C in the Ross Sea and

−1.5°C in the Weddell Sea [*Jacobs et al.*, 1985; *Foldvik et al.*, 1985]. It is also much better oxygenated than the CDW below the pycnocline.

[55] The final stage of the conversion takes place on the Antarctic continental shelves where dense shelf waters have a residence time of several years [*Jacobs et al.*, 1985; *Foldvik et al.*, 1985]. Much of the heat given up to the atmosphere during the production of dense shelf waters is due, not to cooling, but to the latent heat of fusion during ice formation in coastal polynyas [*Gordon*, 1991]. This is important because heat lost to the atmosphere from freezing does not depress the pCO_2. Given the residence time and the limited amount of cooling taking place on the shelves during the final stage of deep-water formation, one does not expect much local enhancement of the pCO_2 deficit.

[56] CDW is a mixture of NADW, AABW itself, and aged Indian and Pacific deep water [*Broecker et al.*, 1985]. We assume here that CDW approaches Antarctica with a preformed solubility-induced pCO_2 deficit that is acquired from its NADW and AABW components. The deficit in new NADW was shown previously to be about 60–70 ppm. The deficit in AABW is unknown. By our reckoning, the net effect of bottom water formation in the south is to erase some of the preformed pCO_2 deficit; that is, exposure of bottom water precursors to the atmosphere in the open ocean and then on the shelves should more than compensate for any local cooling and should act to raise deep TCO_2 concentrations toward full solubility. This means that the average solubility-induced pCO_2 deficit in southern bottom water should be less than the 60–70 ppm deficit derived in the North Atlantic, perhaps 30–40 ppm. The average pCO_2 deficit for the deep ocean would then be a combination of 60–70 ppm deficit in NADW and the estimated 30–40 ppm deficit in AABW, perhaps 50–60 ppm.

6.2. Relative Merit of Box Models and GCMs

[57] *Bacastow* [1996] and *Archer et al.* [2000] argue that box models are deficient in the way they represent the thermal partitioning of CO_2. Given the performance of the two models examined here, one would say that neither model is more deficient than the other. An average pCO_2 deficit for the deep ocean of 50–60 ppm lies halfway between the 26 ppm pCO_2 deficit in the three-box model and the 100 ppm pCO_2 deficits generated by the POBM in the Southern Ocean. What does this say about the two models?

[58] Gas exchange is clearly too efficient in the three-box model. The 15% area given over to the polar box is too large to capture the CO_2 disequilibrium seen in the oceanic pCO_2 data. On the other hand, the area of the polar box is easily changed. According to Figure 4, the pCO_2 deficit in the polar box comes into agreement with our 50–60 ppm target deficit if the area of the polar box is reduced from 15% to 6%. With a 6% polar area, the surface to deep difference in TCO_2 in the three-box model shrinks to 120 μmol/kg. This makes the solubility pump about 15% weaker.

[59] Gas exchange in the Southern Ocean in the POBM is not efficient enough. Southern bottom-water formation in the real ocean evolves along an advective pathway: CDW comes to the surface around Antarctica, is cooled, and then moves onto the shelves where it descends to the abyss again in sinking plumes. This mode of deep-water formation spreads the air-sea equilibration process out over space and time. Level-coordinate GCMs like the POBM do not represent this process very well [*Winton et al.*, 1998]. Cooling in the POBM tends to occur in deep convective columns as shown in Figure 5. Heat removal, deep-water formation, and CO_2 equilibration must all occur in the same limited areas at the same time. This mode of deep-water formation tends to increase the pCO_2 deficit for deep water over the deficit being set in the North Atlantic. This kind of deep convection is reduced in more up-to-date GCMs run with the Gent-McWilliams eddy transport parameterization and seasonal forcing but an advective pathway does not materialize in its place [*Gnanadesikan et al.*, 2002]. Solubility-induced pCO_2 deficits in the Southern Ocean remain very high.

[60] To add insult to injury, convection in the POBM occurs under a fixed sea-ice cover which reduces the rate of gas exchange and the degree of air-sea equilibration. There may be circumstances where a strong sea-ice limitation on gas exchange might be reasonable (e.g., where convection is driven by brine rejection under slowly growing thick ice). However, given the role of coastal and open-ocean polynyas in convective areas in the real Southern Ocean, one should not assume that the water in these convecting regions cannot exchange CO_2 with the atmosphere. The use of sea-ice climatologies to limit gas exchange probably leads to a serious underestimation of the strength of the solubility pump in many GCMs.

7. Conclusions

[61] With very fast gas exchange rates, the deep ocean would hold as much CO_2 as thermodynamic equilibrium allows. With finite gas exchange rates the deep ocean holds less CO_2. This limitation on CO_2 solubility comes about mainly through the pCO_2 deficit carried into the interior in new deep water. The initial pCO_2 deficit is minimal (∼25 ppm) in simple box models that have large polar boxes. Initial pCO_2 deficits are much larger in the GCM-based Princeton Ocean Biogeochemistry Model (70 ppm in the north, 100 ppm in the south). Finite gas exchange rates in the POBM give rise to larger deficits because of the polar areas available for the physical exchange of surface and deep water are small and tend to be ice covered.

[62] The solubility-induced pCO_2 deficit in new North Atlantic Deep Water appears to be about 60–70 ppm. This deficit is produced by the high-latitude cooling associated with the poleward flow of surface and near-surface waters in the North Atlantic. The formation of bottom water in the Southern Ocean involves much less cooling. We surmise that the net effect of deep-water formation in the south is to reduce the average pCO_2 deficit for the deep ocean as a whole to perhaps 50–60 ppm. This puts the strength of the solubility pump in the real ocean about halfway between the pump strengths in the standard three-box model and the POBM. A polar pCO_2 deficit of 50–60 ppm reduces the thermal TCO_2 difference between surface water and deep

water to roughly 120 μmol/kg. This suggests that the solubility pump in the real ocean is responsible for about 35% of the surface to deep TCO_2 difference instead of 50% at full solubility.

[63] This paper was motivated by observations by *Bacastow* [1996], *Broecker et al.* [1999], and *Archer et al.* [2000] that simple box models partition less CO_2 into cold deep water than GCMs. These authors assumed that the thermal partitioning in simple box models must be deficient because these models are missing key circulation and mixing features that are present in the real ocean. Missing circulation and mixing features are not the issue. The main difference is the degree of air-sea equilibration in new deep water. In this regard, new deep water in the three-box model seems to be too well equilibrated while new southern deep water in GCMs would seem to be too poorly equilibrated. The solubility pump in the three-box model can be made more realistic with a simple reduction in the area of its polar box. A more realistic treatment of the solubility pump in GCMs requires a more realistic treatment of bottom water formation in the Southern Ocean that better represents the last stages of air-sea contact on the Antarctic continental shelves.

[64] **Acknowledgments.** The authors would like to thank Roberta Hotinski and Katsumi Matsumoto for their internal reviews of this manuscript. We would like to acknowledge a series of fruitful discussions with David Archer that helped refine a number of the main points of the paper and would like to thank Niki Gruber for his external review. The work of Cathy Raphael and Jeff Varanyak in preparing the figures is also appreciated. A.G. and J.L.S. would like to acknowledge support for the Carbon Modeling Consortium from NOAA's Office of Global Programs (grant NA96GP0312).

References

Archer, D. E., G. Eshel, A. Winguth, W. Broecker, R. Pierrehumbert, M. Tobis, and R. Jacob, Atmospheric pCO_2 sensitivity to the biological pump in the ocean, *Global Biogeochem. Cycles*, *14*, 1219–1230, 2000.

Bacastow, R. B., The effect of temperature change of the warm surface waters of the oceans on atmospheric CO_2, *Global Biogeochem. Cycles*, *10*, 319–333, 1996.

Broecker, W. S., T. Takahashi, and T. Takahashi, Sources and flow patterns of deep-ocean waters as deduced from potential temperature, salinity, and initial phosphate concentration, *J. Geophys. Res.*, *90*, 6925–6939, 1985.

Broecker, W., J. Lynch-Stieglitz, D. Archer, M. Hoffmann, E. Maier-Reimer, O. Marchal, T. Stocker, and N. Gruber, How strong is the Harvardton-Bear constraint?, *Global Biogeochem. Cycles*, *13*, 817–821, 1999.

Bryan, K., and L. Lewis, A water mass model of the World Ocean, *J. Geophys. Res.*, *84*, 2503–2517, 1979.

Department of Energy, DOE handbook of methods for the analysis of the various parameters of the carbon dioxide system in seawater, version 2, edited by A. G. Dickson and C. Goyet, *ORNL/CDIAC-74*, Washington, D. C., 1994.

Foldvik, A., T. Gammelsrod, and T. Torrensen, Circulation and water masses on the southern Weddell Sea Shelf, in *Oceanology of the Antarctic Continental Shelf*, *Antarctic Res. Ser.*, vol. 43, edited by S. Jacobs, pp. 5–20, AGU, Washington, D. C., 1985.

Gnanadesikan, A., R. D. Slater, N. Gruber, and J. L. Sarmiento, Oceanic vertical exchange and new production: A comparison between models and observations, *Deep Sea Res., Part II*, *49*, 363–401, 2002.

Gordon, A. L., Two stable modes of Southern Ocean winter stratification, in *Deep Convection and Deep Water Formation in the Oceans*, edited by P. C. Chu and J. C. Gascard, *Elsevier Oceanogr. Ser.*, vol. 57, pp. 17–35, Elsevier Sci., New York, 1991.

Gruber, N., and J. L. Sarmiento, Large-scale biogeochemical/physical interactions, in *The Sea, Biological/Physical Interactions*, vol. 12, edited by A. R. Robinson, J. J. McCarthy, and B. J. Rothschild, pp. 337–399, John Wiley, New York, 2002.

Jacobs, S. S., R. G. Fairbanks, and Y. Horibe, Origin and evolution of water masses near the Antarctic continental margin: Evidence from $H_2{}^{18}O/H_2{}^{16}O$ ratios in seawater, in *Oceanology of the Antarctic Continental Shelf*, *Antarctic Res. Ser.*, vol. 43, edited by S. Jacobs, pp. 59–85, AGU, Washington, D. C., 1985.

Martinson, D. G., and R. A. Ianuzzi, Antarctic ocean-ice interactions: Implications from ocean bulk property distributions in the Weddell gyre, in *Antarctic Sea Ice: Physical Processes, Interactions, and Variability*, *Antarctic Res. Ser.*, vol. 74, edited by M. O. Jeffries, pp. 243–271, AGU, Washington, D. C., 1998.

Mauritzen, C., Production of dense overflow waters feeding the North Atlantic across the Greenland-Scotland Ridge, 2, An inverse model, *Deep Sea Res., Part I*, *43*, 807–835, 1996.

Murnane, R. J., J. L. Sarmiento, and C. LeQuere, Spatial distribution of air-sea CO_2 fluxes and the interhemispheric transport of carbon by the oceans, *Global Biogeochem. Cycles*, *13*, 287–305, 1999.

Orsi, A. H., G. C. Johnson, and J. L. Bullister, Circulation, mixing, and production of Antarctic Bottom Water, *Prog. Oceanogr.*, *43*, 55–109, 1999.

Sarmiento, J. L., and J. R. Toggweiler, A new model for the role of the oceans in determining atmospheric CO_2, *Nature*, *308*, 621–624, 1984.

Sarmiento, J. L., P. Monfray, E. Maier-Reimer, O. Aumont, R. J. Murnane, and J. C. Orr, Sea-air CO_2 fluxes and carbon transport: A comparison of three ocean general circulation models, *Global Biogeochem. Cycles*, *14*, 1267–1281, 2000.

Schmitz, W. J., and P. L. Richardson, On the sources of the Florida Current, *Deep Sea Res.*, *38*, Suppl., S379–S409, 1991.

Siegenthaler, U., and T. Wenk, Rapid atmospheric CO_2 variations and ocean circulation, *Nature*, *308*, 624–626, 1984.

Takahashi, T., T. T. Takahashi, and S. C. Sutherland, An assessment of the role of the North Atlantic as a CO_2 sink, *Philos. Trans. R. Soc. London, Ser. B*, *348*, 143–152, 1995.

Toggweiler, J. R., Variation of atmospheric CO_2 by ventilation of the ocean's deepest water, *Paleoceanography*, *14*, 571–588, 1999.

Toggweiler, J. R., and J. L. Sarmiento, Glacial to interglacial changes in atmospheric carbon dioxide: The critical role of ocean surface water in high latitudes, in *The Carbon Cycle and Atmospheric CO_2: Natural Variations Archean to Present*, *Geophys Monogr. Ser.*, vol. 32, edited by E. T. Sundquist and W. S. Broecker, pp. 163–184, AGU, Washington, D. C., 1985.

Toggweiler, J. R., R. Murnane, S. Carson, A. Gnanadesikan, and J. L. Sarmiento, Representation of the carbon cycle in box models and GCMs, 2, Organic pump, *Global Biogeochem. Cycles*, doi:10.1029/2001GB001841, in press, 2003.

Volk, T., and M. I. Hoffert, Ocean carbon pumps: Analysis of relative strengths and efficiencies in ocean-driven atmospheric CO_2 changes, in *The Carbon Cycle and Atmospheric CO_2: Natural Variations Archean to Present*, *The Carbon Cycle and Atmospheric CO_2: Natural Variations Archean to Present*, *Geophys. Monogr. Ser.*, vol. 32, edited by E. T. Sundquist and W. S. Broecker, pp. 99–110, AGU, Washington, D. C., 1985.

Weiss, R. F., F. A. Van Woy, and P. K. Salemeh, Surface water and atmospheric carbon dioxide and nitrous oxide observations by shipboard automated gas chromatography: Results from expeditions between 1977 and 1990, report, 121 pp., Carbon Dioxide Inf. Anal. Cent., Oak Ridge Natl. Lab., Oak Ridge, Tenn., 1992.

Winton, M., R. Hallberg, and A. Gnanadesikan, Simulation of density-driven frictional downslope flow in z-coordinate ocean models, *J. Phys. Oceanogr.*, *28*, 2163–2174, 1998.

S. Carson, A. Gnanadesikan, and J. R. Toggweiler, Geophysical Fluid Dynamics Laboratory, National Oceanic and Atmospheric Administration, P.O. Box 308, Princeton, NJ 08648, USA. (sc@gfdl.noaa.gov; a1g@gfdl.noaa.gov; jrt@gfdl.noaa.gov)

R. J. Murnane, Risk Prediction Initiative, Bermuda Biological Station for Research, Inc., P.O. Box 405, Garrett Park, MD 20896, USA. (rmurnane@bbsr.edu)

J. L. Sarmiento, Atmospheric and Oceanic Sciences Program, Princeton University, P.O. Box CN710, Princeton, NJ 08544-0710, USA. (jls@princeton.edu)